Journal of Computational Neuroscience 18, 311–321, 2005

Dynamics of the Instantaneous Firing Rate in Response to Changes in Input Statistics

NICOLAS FOURCAUD-TROCMÉ*
Department of Mathematics, University of Pittsburgh, Center for Neural Basis of Cognition, Pittsburgh, PA 15213, USA
fourcaud@pitt.edu

NICOLAS BRUNEL
Laboratory of Neurophysics and Physiology, UMR8119 CNRS - Université René Descartes, 45 Rue des Saints Pères, 75270 Paris Cedex 06, France
nicolas.brunel@univ-paris5.fr

Received December 7, 2004; Revised January 5, 2005; Accepted January 11, 2005

Abstract. We review and extend recent results on the instantaneous firing rate dynamics of simplified models of spiking neurons in response to noisy current inputs. It has been shown recently that the response of the instantaneous firing rate to small amplitude oscillations in the mean inputs depends in the large frequency limit f on the spike initiation dynamics. A particular simplified model, the exponential integrate-and-fire (EIF) model, has a response that decays as $1/f$ in the large frequency limit and describes very well the response of conductance-based models with a Hodgkin-Huxley type fast sodium current. Here, we show that the response of the EIF instantaneous firing rate also decays as $1/f$ in the case of an oscillation in the variance of the inputs for both white and colored noise. We then compute the initial transient response of the firing rate of the EIF model to a step change in its mean inputs and/or in the variance of its inputs. We show that in both cases the response speed is proportional to the neuron stationary firing rate and inversely proportional to a 'spike slope factor' Δ_T that controls the sharpness of spike initiation: as $1/\Delta_T$ for a step change in mean inputs, and as $1/\Delta_T^2$ for a step change in the variance in the inputs.

Keywords: integrate-and-fire neuron, noise, dynamical response, spiking mechanism

1. Introduction

Cortical neurons *in vivo* receive a massive amount of background synaptic activity, that induces large fluctuations of the membrane potential (see e.g., Destexhe and Paré, 1999; Anderson et al., 2000). This synaptic bombardment is often described by the sum of a deterministic (average) current $\mu(t)$, plus a Gaussian noise term with variance $\sigma(t)$ and temporal correlation τ_s. Given this stochastic environment, the neuronal output is typically characterized by the instantaneous firing rate (or firing probability) $\nu(t)$. The question of how the instantaneous firing rate depends on the statistics of neuronal inputs (both in stationary and non-stationary conditions) in these conditions has been a central question in theoretical neuroscience in recent years. Three basic quantities of interest have been considered:

- The stationary firing rate ν_0 in response to stationary input statistics (μ_0, σ_0);

*To whom correspondence should be addressed.

- The dynamical linear response (susceptibility, or transmission function) of the firing rate to changes of average input current at frequency f;
- The dynamical linear response of the firing rate to changes of the variance of the input current at frequency f.

The leaky integrate-and-fire neuron (Lapicque, 1907; Knight, 1972; Tuckwell, 1988) has been the model of choice for such investigations, due to its simplicity. The main results obtained on this model are the following:

- The stationary firing rate ν_0 increases monotonically with both μ_0 and σ_0, and either decreases monotonically with τ_s (in the subthreshold range) or first decreases and then increases with τ_s (in the suprathreshold range) (Brunel and Sergi, 1998; Moreno and Parga, 2004).
- The behavior of the firing rate response to changes in mean inputs depends markedly on both the amplitude of noise and temporal correlations present in the noise (Knight, 1972; Gerstner, 2000; Brunel et al., 2001; Lindner and Schimansky-Geier, 2001; Fourcaud and Brunel, 2002). In the 'suprathreshold' (low noise and DC current above current threshold) regime the dynamical response features resonances at input frequencies which are integer multiple of the neuron stationary firing rate. These resonances disappear in the 'subthreshold' (high noise and/or DC current below threshold) regime. The response of the neurons to high frequency f oscillations in mean input current decrease as $1/\sqrt{f}$ in the presence of white noise and is finite in the presence of colored noise.
- The instantaneous firing rate is directly proportionnal to the input variance and consequently the firing rate response to changes in variance has an instantaneous component (Silberberg et al., 2004; Lindner and Schimansky-Geier, 2001).

More recent studies have shown however that the high frequency properties of the linear response (and therefore the short time behavior of the firing rate response to dynamical stimuli) depend in a sensitive way on the mechanism leading to spike emission (Fourcaud-Trocmé et al., 2003). Hence, the LIF might not be the appropriate model to investigate fast firing rate transients. Fourcaud-Trocme et al. (2003) have introduced a new model, the exponential integrate-and-fire model, that captures both qualitatively and quantitatively the properties of the linear response of some Hodgkin-Huxley type models.

Here, we first start by reviewing the properties of the linear response of the firing rate of the EIF model in response to change in mean inputs. Then, we describe the properties of the response to changes in the variance of synaptic inputs, and compute the initial transient firing rate response to a step change in both mean and variance of inputs. We then discuss under which conditions neurons respond faster to step changes in their mean inputs or changes in the variance. Finally, in the discussion, we compare the results obtained in the models with available experimental data.

2. Models and Methods

2.1. Models

Non-linear IF (NLIF) neuronal models are one variable models that generalize the classic LIF model by including an additional non-linear current ψ which leads to a divergence of the potential toward infinity in a finite time (Ermentrout and Kopell, 1986; Ermentrout, 1996; Fourcaud-Trocmé et al., 2003). The action potential time is defined as the time the potential reaches infinity. The equation describing the dynamics of the membrane potential of these models is:

$$C\frac{dV}{dt} = -g_L(V - V_L) + \psi(V) + I(t) \qquad (1)$$

where C and g_L are the neuron capacitance and conductance, ψ is the non-linear current leading to spike generation and I is the external input current. When a spike is emitted (i.e. at the time at which the voltage reaches infinity), the voltage is reset at the potential V_r.

One classic example of such family of models is the quadratic integrate-and-fire model (QIF, Ermentrout and Kopell, 1986; Ermentrout, 1996; Hansel and Mato, 2003) defined by:

$$\psi(V) = \frac{g_L}{2\Delta_T}(V - V_T)^2 + g_L(V - V_L) \qquad (2)$$

The exponential integrate-and-fire model (Fourcaud-Trocmé et al., 2003) is defined by:

$$\psi(V) = g_L\Delta_T \exp\left(\frac{V - V_T}{\Delta_T}\right) \qquad (3)$$

In both models, V_T is the *voltage threshold*, i.e. the largest steady voltage at which the neuron can be

maintained by a constant input current, and Δ_T is the *spike slope factor* which measures the sharpness of the spike (sharp initiation for small Δ_T). In the limit $\Delta_T \to 0$ in the EIF model, the standard LIF is recovered (the 'spike-generating' current ψ becomes infinite above the voltage threshold V_T).

The parameter Δ_T is related to the time it takes for the model to emit a spike from an initial voltage of V_T: in the limit $\Delta_T \to 0$, we can show that for an input current $\mu = \frac{I}{g_L} > V_T - V_L$, the time from threshold to spike emission is, for the EIF model:

$$T \sim \frac{\tau_m \Delta_T}{(\mu - V_T + V_L)} \ln\left(\frac{\mu - V_T + V_L + \Delta_T}{\Delta_T}\right)$$

Hence the time from the threshold to spike emission behaves as $\Delta_T |\log(\Delta_T)|$ when Δ_T is small.

In this study we mostly focus on the EIF model which captures the dynamical properties of neurons where the activation variable of the current responsible for the spike initiation (the fast sodium current) can be well described by an exponential close to spike threshold, as in the standard Hodgkin-Huxley model (see Fourcaud-Trocmé et al., 2003). In particular, all the simulations presented here were done using the EIF model, using the numerical methods described in Fourcaud-Trocmé et al. (2003). The model parameters are chosen to reproduce accurately the dynamics of a type I model described by Wang and Buzsáki (1996). These parameters are: $\tau_m = C/g_L = 10$ ms, $V_T = -59.9$ mV, $\Delta_T = 3.48$ mV, $V_L = -65$ mV and $V_r = -68$ mV. This gives a current threshold $\mu_T = I_T/g_L = 1.62$ mV. We also include a refractory period $\tau_{\text{ref}} = 1.7$ ms to take into account the spike width.

Following standard practice, we use the diffusion approximation to describe background synaptic inputs (Ttuckwell, 1988). The input current is given by the sum of a deterministic mean and a Gaussian noise term. In the simplest case where the synapses are assumed to be instantaneous (and therefore the temporal correlations of the noise are neglected), we have:

$$I(t) = g_L \mu(t) + \sigma(t)\sqrt{C g_L}\eta(t) \tag{4}$$

where $\mu(t)$ and $\sigma(t)$ (both in mV units) describe the mean and the variance of the input current, and $\eta(t)$ is a Gaussian white noise of unitary variance. When synapses have a finite decay time, $\eta(t)$ is a colored noise, i.e. a low-pass filtered white noise. Throughout this paper, we consider for simplicity white noise, except when specified otherwise.

2.2. *Methods*

From the Langevin Eq. (1) and (4), we can derive the Fokker-Planck equation which describes the evolution of the membrane potential probability density function (p.d.f.) $P(V, t)$,

$$\tau_m \frac{\partial P}{\partial t} = \frac{\sigma(t)^2}{2}\frac{\partial^2 P}{\partial V^2} - \frac{\partial}{\partial V}\big(F(V) + \mu(t)\big)P \tag{5}$$

where $\tau_m = C/g_L$ is the membrane time constant and $F(V) = -(V - V_L) + \psi(V)/g_L$. The firing rate of the neuron is given by the probability flux at the spike emission threshold, i.e. its limit when the voltage goes to infinity for NLIF models:

$$\nu(t) = \lim_{V \to +\infty} J_V(V, t) \tag{6}$$

where the probability flux J_V is given by:

$$J_V(V, t) = \frac{F(V) + \mu(t)}{\tau_m} P(V, t) - \frac{\sigma(t)^2}{2\tau_m}\frac{dP}{dV}(V, t).$$

The reset of the voltage to V_r after a spike emission is taken into account by requiring that

$$J_V(V_r^+, t) = J_V(V_r^-, t) + \nu(t). \tag{7}$$

Another boundary condition is:

$$\lim_{V \to -\infty} J_V(V, t) = 0 \tag{8}$$

With constant inputs, the stationary solution of Eq. (5) can be computed by setting its l.h.s to zero. Finding the solution of Eq. (5) for time-varying inputs is however a difficult problem in general. To overcome this problem, we restrain ourselves to the analysis of the firing rate response to small time-dependent perturbations of μ or σ. Neglecting non-linear terms in the response, we can take advantage of Fourier analysis, and fully characterize the dynamics of the system by computing the response to sinusoidal inputs at all frequencies. Thus, the inputs take the form:

$$\mu(t) = \mu_0 + \mu_1 \cos(\omega t) \tag{9}$$

$$\sigma(t) = \sigma_0 + \sigma_1 \cos(\omega t) \tag{10}$$

where $\omega = 2\pi f$. Throughout this paper, the subscript 0 always refers to the stationary component of any variable, whereas the subscript 1 refers to the oscillatory

part of the same variable. For all variables x, we assume $x_1 \ll x_0$. Neglecting non-linear terms in the response of the system, the p.d.f of the voltage and the firing rate to oscillatory mean (resp. variance) are:

$$P(V,t) = P_0(V) + \Re\left[P_1^{\mu,\sigma}(V,\omega)e^{i\omega t}\right] \quad (11)$$

$$\nu(t) = \nu_0 + \Re\left[\nu_1^{\mu,\sigma}(\omega)e^{i\omega t}\right] \quad (12)$$

where $\Re[\cdot]$ denotes the real part of a complex variable. The superscript μ (resp. σ) refers to the case where the input mean (resp. the variance) oscillates.

3. Results

This section contains both a review of results described in Fourcaud-Trocmé et al. (2003) (stationary firing rate and response to oscillatory mean input) together with new results (response to oscillatory variance, response to steps in both mean and variance).

3.1. Stationary Firing Rate

The stationary firing rate of the neuron ($\mu_1 = \sigma_1 = 0$) is obtained from Eq. (5) by setting $\partial P/\partial t = 0$, together with the normalization condition $\int P(V)\,dV = 1$ (Fourcaud-Trocmé et al., 2003). It yields:

$$\nu_0 = \left\{\tau_{\text{ref}} + \frac{2\tau_m}{\sigma_0^2}\int_{-\infty}^{+\infty} dV\left[\int_{\max(V,V_r)}^{+\infty} \times \exp\left(-\frac{2}{\sigma_0^2}\int_V^u (F(x)+\mu_0)dx\right)du\right]\right\}^{-1} \quad (13)$$

The firing rate ν_0 is plotted as a function of μ_0 (f-I curve) in the upper left panel of Fig. 1. It is plotted as a function of σ_0 (f-σ curve) in the upper right panel. In absence of noise, the f-I curve has the $\sqrt{\mu_0 - V_T}$ behavior characteristic of type-I neurons close to threshold. The firing rate is a monotonically increasing function of σ_0 for subthreshold mean inputs, while for sufficiently suprathreshold inputs the firing rate decreases with noise at low values of σ_0, reaches a minimum, and then increases with noise at high values of σ_0. Equation (13) can be simplified to a single integral in the particular case of the quadratic neuron (Lindner et al., 2003; Brunel and Latham, 2003).

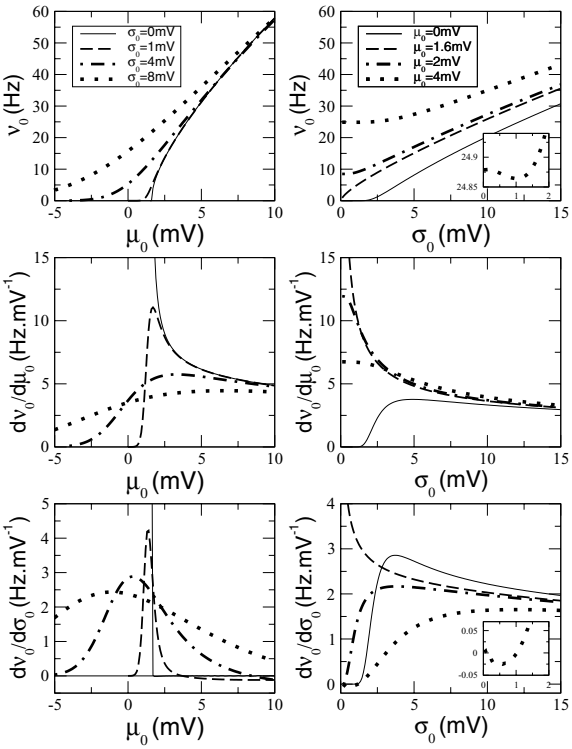

Figure 1. EIF firing rate and low input frequency response as a function of input mean (left column) and input variance (right column). Upper panels: stationary firing rate. Middle panels: derivative with respect to the input current mean. Lower panels: derivative with respect to the input current variance. In the right column, the insets are an enlargement of the low noise region for the parameter $\mu_0 = 4$ mV. It shows the negative derivative with respect to σ_0 of the firing rate in this region.

3.2. Linear Response for Low Input Frequencies

For inputs that vary on a slow enough time scale, the firing rate response can be obtained directly from the f-I curve, since the firing rate follows adiabatically these slow changes. Hence,

$$\nu_1^{\mu}(\omega \to 0) = \mu_1 \frac{\partial \nu_0}{\partial \mu_0}, \quad (14)$$

and

$$\nu_1^{\sigma}(\omega \to 0) = \sigma_1 \frac{\partial \nu_0}{\partial \sigma_0} \quad (15)$$

It can be shown from Eq. (13) that $\partial\nu_0/\partial\mu_0$ is always strictly positive. However, $\partial\nu_0/\partial\sigma_0$ can be either positive or negative depending on the shape of the function

ψ. In the EIF model, we have seen that the rate decreases with σ_0 when μ_0 is sufficiently above the current threshold and the noise level is low (see insets in the right column of Fig. 1). The consequence is that the firing rate response to a low frequency oscillation in the input variance σ has a phase lag equal to π in these conditions.

The four lower panels of Fig. 1 show the low frequency responses as a function of both μ_0 and σ_0. Note that the system is more susceptible to low-frequency changes in its inputs (in both mean and variance) when it is close to threshold, except when noise is very strong. When the mean inputs are subthreshold, the susceptibility (for both mean and variance) is maximal at a non-zero value of the noise σ_0. However, for suprathreshold mean inputs, the susceptibility with respect to low-frequency changes in the mean input decays monotonically with σ_0 while for oscillations in the variance, there is still a maximal response at a non-zero value of σ_0.

3.3. *High Input Frequency Limit*

In the limit of high frequency inputs, we can determine the firing rate susceptibility using an expansion in $1/\omega$. Inserting Eq. (11) in the FP equation (Eq. (5)) gives at first order in μ_1, σ_1:

$$i\omega\tau_m P_1 = \frac{\sigma_0^2}{2}\frac{\partial^2 P_1}{\partial V^2} - \frac{\partial}{\partial V}(F+\mu_0)P_1 - \mu_1\frac{\partial P_0}{\partial V} + \sigma_1\sigma_0\frac{\partial^2 P_0}{\partial V^2} \tag{16}$$

Then, in the limit $\omega \to \infty$, it can be shown that

$$P_1(V,\omega) \sim_{\omega\to\infty} \frac{1}{i\omega\tau_m}\left[-\mu_1\frac{\partial P_0}{\partial V} + \sigma_1\sigma_0\frac{\partial^2 P_0}{\partial V^2}\right] \tag{17}$$

Using the boundary condition (6) we obtain for the firing rate

$$\begin{aligned}\nu_1(\omega) &= \lim_{V\to+\infty}\left[\frac{F(V)+\mu_0}{\tau_m}P_1(V,\omega) - \frac{\sigma_0^2}{2\tau_m}\frac{\partial P_1}{\partial V}(V,\omega) + \frac{\mu_1}{\tau_m}P_0(V) + \frac{\sigma_0\sigma_1}{\tau_m}\frac{\partial P_0}{\partial V}(V)\right] \\ &= \lim_{V\to+\infty}\left[\frac{F(V)}{\tau_m}P_1(V,\omega)\right]\end{aligned} \tag{18}$$

where in the last equality, we have used the fact that $F(V)$ goes to infinity at large V.

Finally, we combine Eqs. (17) and (18) together with

$$P_0(V) \sim_{V\to\infty} \frac{\nu_0\tau_m}{F(V)}, \tag{19}$$

to compute the high frequency response to a fluctuation of the mean or the variance of the input current.

High Frequency Oscillation in Mean Inputs. The first term in the expansion in $1/\omega$ of ν_1 in the case $\mu_1 > 0, \sigma_1 = 0$ gives:

$$\nu_1^\mu(\omega) \approx \frac{\mu_1\nu_0}{i\omega\tau_m}\lim_{V\to\infty}\frac{F'(V)}{F(V)} = \frac{\mu_1\nu_0}{i\omega\tau_m}\lim_{V\to\infty}\frac{\psi'(V)}{\psi(V)} \tag{20}$$

Fourcaud-Trocmé et al. (2003) showed that this result holds for both white and colored noise inputs (corresponding to non-instantaneous synapses), and for multiplicative noise (corresponding to conductance-based synapses). Thus, the qualitative behavior of the high frequency response to a fluctuation of the mean of the input current for the NLIF models *is independent of the noise level or model*, in contrast with the LIF model. Rather, it is determined by the shape of the function leading to the spike emission $\psi(V)$. Intuitively, the reason is that the spike-generating current completely dominates the dynamics for sufficiently large voltages, and the dynamics becomes independent of the fluctuations at such large voltages.

In particular, for the EIF model we find:

$$\nu_1^\mu(\omega) \approx \frac{\mu_1\nu_0}{i\omega\tau_m\Delta_T} \tag{21}$$

yielding a phase lag of $\pi/2$ at high frequency. Hence, the response is inversely proportional to both τ_m and Δ_T. Intuitively, the faster a neuron can fire a spike, the better it can respond to high frequency inputs.

Note that for the QIF model, as well as for any polynomial spike-generating current ψ, the first order term of the asymptotic expansion vanishes. Hence we need to compute higher order terms. For the QIF model, we obtain

$$\nu_1^\mu(\omega) \approx -\frac{\mu_1\nu_0}{(\omega\tau_m)^2\Delta_T} \tag{22}$$

yielding a phase lag of π at high frequency. Note the qualitative difference between the behaviors of EIF

$(1/f)$ and QIF $(1/f^2)$ models. Hence, the functional form of the voltage dependence of the activation variable of fast sodium currents has strong effects on how a neuron can follow fast frequency inputs.

High-Frequency Oscillation in Variance. Likewise, we can compute the first order term of the expansion in $1/\omega$ of NLIF models in response to a high frequency oscillation of the variance of the input current ($\sigma_1 > 0$, $\mu_1 = 0$). We obtain:

$$\nu_1^\sigma(\omega) \approx \frac{\sigma_0\sigma_1\nu_0}{i\omega\tau_m} \lim_{V\to\infty} \frac{2\psi'(V)^2 - \psi''(V)\psi(V)}{\psi(V)^2} \quad (23)$$

Once again, there is a striking difference with the simple LIF model where this high frequency response is finite (Silberberg et al., 2004; Lindner and Schimansky-Geier, 2001). In NLIF models, Eq. (23) shows that, as for an oscillation of μ, the intrinsic current leading to the spike generation $\psi(V)$ determines the high frequency response.

In particular, we find for the EIF model:

$$\nu_1^\sigma \approx \frac{\sigma_0\sigma_1\nu_0}{i\omega\tau_m\Delta_T^2} \quad (24)$$

As in the case of a fluctuation of μ, we can obtain the QIF response to fluctuations of σ by going to higher orders (up to the third order here):

$$\nu_1^\sigma \approx \frac{2\sigma_0\sigma_1\nu_0}{(i\omega\tau_m)^3\Delta_T} \quad (25)$$

As for the case of the oscillation in the mean, the $1/f$ asymptotic behavior of the EIF model holds for both white and colored noise inputs. However, the QIF high frequency response to an input variance oscillation is proportional to $1/f^2$ in the case of colored noise inputs (Naundorf et al., 2003).

Comparison Between Responses to Mean and Variance High Frequency Oscillations. In the EIF model, the high frequency behavior of both ν_1^μ and ν_1^σ are qualitatively similar—they both decay as $1/f$ at high frequency. On the other hand, the QIF model is more susceptible to very fast changes in μ ($1/f^2$ attenuation) than to very fast changes in σ ($1/f^3$ attenuation), contrary to the LIF neuron.

In the EIF model, the high frequency response to oscillatory variance has an additional factor of σ_0/Δ_T with respect to the response to oscillatory mean. Hence, for $\Delta_T \ll \sigma_0$ (very sharp spike initiation and/or large background fluctuations), the system is more susceptible to high-frequency variance fluctuations than to high-frequency mean fluctuations. This $\Delta_T \to 0$ limit is consistent with known results on the LIF neuron (Silberberg et al., 2004; Lindner and Schimansky-Geier, 2001). In the opposite situation $\sigma_0 \ll \Delta_T$, the system is more susceptible to high-frequency fluctuations in the mean than in the variance.

Intuitively, the dependence of the dynamics on Δ_T and σ_0 can be understood from the following arguments: at small noise levels, the EIF model spends most of its time in the region close to the voltage threshold V_T around which the voltage dynamics is well approximated by the QIF model, which we have seen is more susceptible to rapid fluctuations in the mean of the input. However, at high noise levels, the EIF membrane potential visits a large voltage range around V_T and is less sensitive to the dynamics close to threshold. Thus, at high noise levels, the model has a LIF-type behavior, i.e. it responds better to fast fluctuations in the variance than to those in the mean input.

3.4. Full Frequency Range

To obtain the firing rate response of the EIF model at intermediate input frequencies, we performed numerical simulations. Results are shown in Fig. 2. These simulations show that at low noise levels (Fig. 2, upper panels), the response to an oscillation of either μ or σ displays resonances at frequencies multiple of the neuron stationary firing rate ν_0. This is because in this regime the spike emission process is close to periodic at frequency ν_0 and hence it resonates with inputs at frequency multiple of this intrinsic frequency. At high frequency (above about 100 Hz in the upper panels of Fig. 2) the response decays in both cases as $1/f$ according to Eqs. (21) and (24).

At high noise levels, the spike discharge becomes strongly irregular and the response to an oscillation in μ becomes that of a low pass filter (Fig. 2, lower-left panel). On the other hand, the response to an oscillation of σ is that of a band pass filter. The system responds best to intermediate frequency inputs, while both low and high frequency inputs are suppressed. The low input frequency attenuation is similar to that of the LIF neuron, while the high frequency attenuation is induced by the spike-generating mechanism. Note that for both filters we can deduce how the

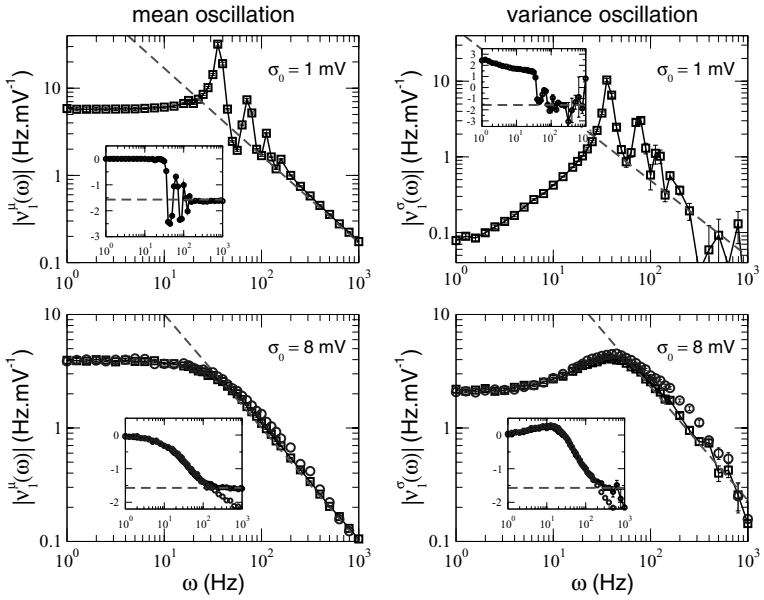

Figure 2. Numerical simulations of the EIF dynamical linear response module (□, phase in insets) over the full range of input frequency. The dashed lines are the analytical results in the high frequency limit (Eqs. (21) and (24)). Left: response to a fluctuation of the input current mean μ. Right: response to an oscillation of the input current variance σ. Upper panels: low noise regime ($\sigma_0 = 1$ mV, $\mu_0 = 6$ mV, $\nu_0 = 37$ Hz). Lower panels: high noise regime ($\sigma_0 = 8$ mV, $\mu_0 = 1.6$ mV, $\nu_0 = 22$ Hz). In the lower panels the EIF response is compared to the response (○) of a type I conductance-based model described by Wang and Buzsáki (1996).

cut-off frequency depends on various parameters from the high frequency behavior (Eqs. (21) and (24)). In particular, for both filters one expects the cut-off frequency to increase as Δ_T becomes small. In the limit $\Delta_T \to 0$ the EIF model becomes equivalent to the LIF model with a threshold equal to V_T: the 'active current' is zero below V_T and infinite above V_T, leading to instantaneous spike generation when the voltage reaches V_T. The linear response to an oscillation of the input mean has a singular limit when $\Delta_T \to 0$: it decays as $1/f^{0/0.5}$ for white/colored noise when $\Delta_T = 0$, while it decays as $1/f$ for any finite Δ_T, with a proportionality constant that goes to infinity as $\Delta_T \to 0$. In practice, for small Δ_T, the response of the EIF neuron tends to the one of the LIF neuron for frequencies $f < f^\star$, where $f^\star$ goes to infinity in the $\Delta_T \to 0$ limit, while the response has a $1/f$ behavior above $f^\star$.

The behavior of the phase shift is also shown in Fig. 2. While the firing rate always lags behind oscillatory mean inputs, it typically displays a phase advance with respect to an oscillatory variance at low frequencies. In fact, the $f \to 0$ limit of the phase can be either 0 or π, depending on the slope of the f-σ curve as described above. Both filters have $\pi/2$ phase lag at high frequency.

In the high noise regime (Fig. 2, lower panels), we show how the EIF response compares with the response of a type I Hodgkin-Huxley type model, the Wang and Buzsáki (1996) model. The EIF model captures accurately the amplitude of the response of the Wang-Buzsáki model to an oscillation of the input mean, as already shown by Fourcaud-Trocmé et al. (2003). It also captures the response to an oscillation of the input variance of the Wang-Buzsáki model, though the agreement between the two models is slightly less good in this case. The phase shifts of both models are very close up to frequencies of the order of 200 Hz. Above this frequency, an additional linear phase lag of the conductance-based model becomes visible. This can be explained by the finite rise time from spike onset to the potential where the spike is counted in this model (Fourcaud-Trocmé et al., 2003).

3.5. *Response to a Step in the Input Mean or Variance*

We next investigate the initial transient firing rate response of the EIF model to a step change of either mean or variance of its input. This is done first analytically

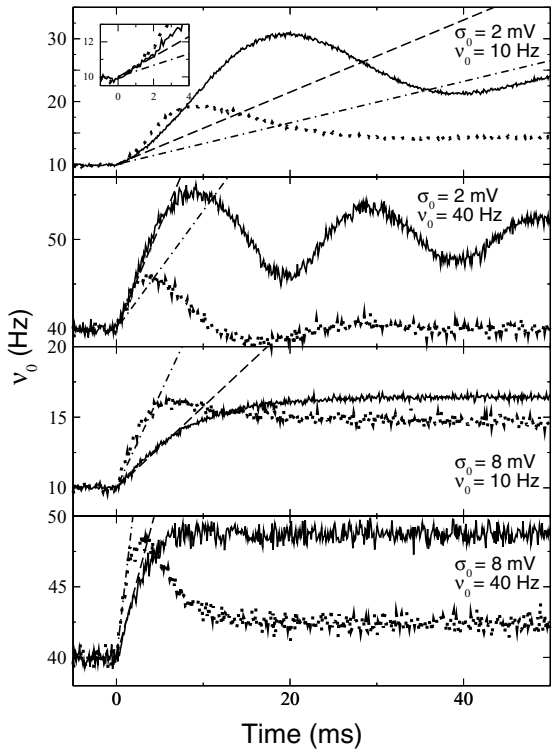

Figure 3. Instantaneous firing rate of the EIF model in response to a step increase of its input mean (full line) or variance (dotted line) of 2 mV at $t = 0$ ms. Each row corresponds to a different initial state of the neuron (different noise level or stationary firing rate). The dashed lines (resp. dotted-dashed lines) are the initial slopes obtained from equations. (27 resp. 28). In the upper panel, the inset is an enlargement of the beginning of the response.

for the short t limit (equivalent to the high f limit, see below), and numerically for the full response (see Fig. 3).

Using $\nu(t) = \nu_0 + (1/(2\pi)) \int d\omega \tilde{H}(\omega)\nu_1(\omega) \exp(i\omega t)$ where $\tilde{H}$ is the Fourier transform of a step increase of mean or variance at time $t = 0$, one can show that the firing rate of the EIF model reacts to a step change in both mean and variance by a discontinuity in the temporal derivative of its firing rate. The initial slope of the response is given by

$$\frac{d\nu}{dt}(0^+) = \lim_{\omega\to\infty} i\omega\nu_1^x(\omega) \tag{26}$$

where x stands for μ or σ depending on which parameter undergoes a step variation. The initial time derivative of the response for the NLIF model can then be simply derived from Eqs. (20) and (23).

In particular, for the EIF model, using Eqs. (21) and (24), we obtain the short time responses:

- for a step in the input mean:

$$\nu(t) \approx \nu_0\left(1 + \frac{\mu_1}{\Delta_T}\frac{t}{\tau_m}\right) \tag{27}$$

- for a step in the input variance:

$$\nu(t) \approx \nu_0\left(1 + \frac{\sigma_1\sigma_0}{\Delta_T^2}\frac{t}{\tau_m}\right) \tag{28}$$

Note that in both cases the initial response is proportional to the neuron initial stationary firing rate. The slope of the response then reflects the behavior of the high frequency dynamical responses: the EIF model responds faster to a step fluctuation of the input mean at low noise levels and/or high spike slope factor ($\sigma_0 < \Delta_T$) and to a step fluctuation of the input variance at high noise level and/or small slope factor ($\sigma_0 > \Delta_T$).

The full response of the EIF model to a step change in various conditions has been obtained using numerical simulations. Results are shown in Fig. 3. At low noise levels, the short time prediction is only accurate in a very brief time interval of order 1ms (see inset in the upper panel of Fig. 3). In this situation, the response grows supralinearly at short times. The presence of resonances in the rate response then translates in a damped oscillatory component of the response to a step before reaching the steady state, which is related to the low frequency response.

In the high noise regime the short-time estimate is accurate for a longer interval (5–10 ms for parameters of Fig. 3). In this case, the firing rate grows sublinearly with time. The EIF response to a mean step fluctuation is simply a low-pass filtered version of the input step (see Fig. 3—lower left panels). On the other hand, the response to a variance step change overshoots the steady state during about the first 10 ms of the response (depending on the model parameters). In that situation, small changes in the variance can be easily detected only in the initial part of the response (in the first 5 ms or so), while changes in the mean can only be detected later (after about 5 ms).

4. Discussion

4.1. Firing Rate Dynamics of the EIF Model

The exponential integrate-and-fire model provides a way to interpolate between the standard LIF model

and type I Hodgkin-Huxley type models. Spike generation in this model is described by a 'spike-generating current' that depends exponentially on voltage. The sharpness of spike initiation can be controlled by the parameter Δ_T: for $\Delta_T = 0$, the LIF is recovered (see Section 2.1 and 3.4), while a value of $\Delta_T \sim 3$ mV permits to fit very well the firing rate response of conductance-based models whose sodium current is as originally described by Hodgkin and Huxley. The instantaneous firing rate response of the EIF model decays as $1/f$ at high frequency in response to oscillations in both mean and variance of its inputs. Other types of non-linearity of the spike-generating current lead to qualitatively different behaviors at high frequency. For example, the QIF neuron has a more pronounced attenuation at high frequency, in response to both mean and variance changes. Results for these different models are summarized in Table 1.

Then, we have considered separately the effects of an oscillation in the mean inputs and in the variance of the inputs. Temporal variations in the firing rate of pre-synaptic neurons will in general provoke changes in both mean and variance of synaptic inputs. The net effect on the post-synaptic firing rate will then depend on the balance between excitation and inhibition. If excitatory pre-synaptic neurons increase their rates, there will be an increase of the post-synaptic firing rate mediated by both mean and variance of inputs. If inhibitory pre-synaptic neurons increase their rates, there can be an increase of the firing rate at short time scales mediated by the resulting change in variance, followed by a decrease of the firing rate at longer times scales mediated by the change in mean.

The EIF model combines advantages of both LIF and HH-type neurons. The LIF model has two principal advantages (1) its firing rate dynamics can be studied analytically; (2) its simplicity permits large scale simulations. However, it lacks many dynamical features exhibited by real neurons, such as a realistic spike generation mechanism. Hodgkin-Huxley models describe the dynamics of real neurons much more accurately, but no analytical treatment is possible, and such models are much more expensive for network simulations. The EIF model provides advantages of both types of model—to some degree analytically tractable, computationnally cheap, and providing an accurate description of the spike generation mechanism of HH-type neurons.

Table 1. Firing rate dynamics of simplified neuronal models at high input frequencies. In all models the firing rate response decays as $1/f^{\alpha}$ at high frequency. The table displays the exponent α, in response to an oscillation of the mean or the variance of the input. In all cases, the corresponding phase shift at high frequency is $\alpha\pi/2$.

Model	α, oscillation in mean (white or colored noise)	α, oscillation in variance (white noise)
LIF	0 (colored noise) 0.5 (white noise)	0
EIF	1	1
QIF	2	3

In the EIF model, the filtering properties have been computed in Fourcaud-Trocmé et al. (2003) and here in both low and high frequency limit. Recently, Naundorf et al. (2003) used a technique that allows to compute the response of the theta neuron (equivalent to the QIF neuron, (equivalent to the QUF neuron, Gutkin and Ermentrout, 1988) and of generalizations of this model at arbitrary frequencies, from a sparse matrix representation of the Fokker-Planck operator. It would be interesting to apply this technique to the EIF model.

The high frequency behaviors obtained in this study apply when spike emission is defined at $V \to \infty$. Defining spike emission at a finite voltage changes the high frequency limit. If resetting occurs at the same finite voltage where spike time is defined, the behavior of the resulting model is qualitatively similar to the LIF neuron. If resetting occurs at infinite voltage, all resulting NLIF models show a $1/f$ decay at high frequency (regardless of the non-linearity), as shown by Naundorf et al. (2004), because the probability flux at the voltage defining spike emission has a non vanishing first order term in the large f expansion (see Eqs. (17) and (18)). However, if the voltage at which spike emission is defined is high, the frequency range affected by the finiteness of the voltage defining spike will be located at unrealistically high values of f. Hence, we expect the scaling laws obtained here to apply in a large frequency range, unless spike emission time is defined at a value close to V_T (relative to Δ_T).

4.2. Other Simplified Model Neurons

Other types of simplified neuron models have been proposed in the literature in recent years. In particular, both adaptation currents (Treves, 1993; Ermentrout, 1998; Ermentrout et al., 2001; van Vreeswijk and Hansel, 2001; La Camera et al., 2004), and currents leading to

subthreshold resonance (Izhikevich, 2001; Richardson et al., 2003; Brunel et al., 2003) can be incorporated in a LIF-type description, or in a NLIF-type description (Izhikevich, 2003), leading to two-variable models that can capture effectively the dynamics of many types of real neurons. These currents do not modify the high frequency filtering properties. However, they profoundly shape the firing rate dynamics at low (compared to the inverse of the relevant time constants) frequencies (Fuhrmann et al., 2002; Richardson et al., 2003; Brunel et al., 2003). The spike response formalism provides an alternative way to describe most such models (Gerstner and Kistler, 2002).

4.3. Simplified Model Neurons vs Real Neurons

We have seen that the EIF model can reproduce accurately the firing rate dynamics of a particular Hodgkin-Huxley type neuron. How do this model, or other simplified models, compare with real neurons? We now review the experimental data available for all the quantities that we have computed in this paper.

Stationary f-I Curve. Tateno et al. (2004) studied f-I curves of cortical neurons (both pyramidal cells and fast-spiking interneurons) in absence of noise. They present clear evidence for the existence of both type I (continuous f-I curve—pyramidal cells) and type II (discontinuous f-I curve—interneurons) behaviors. They showed in particular that type I neurons have a firing rate that increases as a square root of the current beyond threshold, consistent with theoretical type I models. Rauch et al. (2003) studied f-I curves of cortical pyramidal cells in the presence of noise. They showed such curves can be fitted by a simple LIF model with adaptation.

Firing Rate Response to Oscillatory Inputs. Until recently, no published experimental study had to our knowledge measured such a response beyond several tens of Hz. Recently, Koendgen et al. (2004) showed in rat somatosensory cortical neurons that the high frequency linear response to a fluctuation of the input mean decays as $1/\omega^{\alpha}$ with $\alpha > 1$, independently of the noise correlation time constant, with a cutoff frequency of the order of 200 Hz. This behavior is consistent with a NLIF model with a very small Δ_T (very sharp spike), and a non-linearity which is intermediate between exponential and quadratic.

Firing Rate Response to Steps. Silberberg et al. (2004) studied the speed of the response to a step change in the input mean or input variance in neocortical neurons. They found that neurons responded almost instantaneously to a step change of σ and showed that these results could be captured by the LIF model. This is again consistent with a small value of Δ_T in a NLIF model.

The question of which model to use for single neurons is a central question for theorists interested in network modeling, and various paths have been explored over the years. In the traditional Hodgkin-Huxley approach, one has to measure the characteristics of all types of currents present in a neuron, which represents difficult and time-consuming experiments, and leads to complex models. At the other extreme, firing rate models use approximate forms of the f-I curve of real neurons, together with a simple Wilson-Cowan type rate dynamics. The static response is then close to the one of those real neurons, but there is no guarantee that the dynamics will be captured. An intermediate and potentially very fruitful approach to capture firing rate dynamics of real neurons would be to obtain a model that reproduces both f-I curve and linear rate response to both oscillatory mean and variance. We believe that the NLIF neuron models (or generalized versions of it to capture low frequency dynamics) are suitable candidates for such models. The partial data that exists about the linear response properties of cortical neurons indicate that apart from very specific situations (low noise, very high frequencies) their firing rate dynamics seems to be well described by LIF neurons. However, more data is clearly needed to be able to discriminate in a clear way between different models.

Acknowledgments

We are indebted to Alex Roxin and Carl van Vreeswijk for their comments on the manuscript.

References

Anderson JS, Lampl I, Gillespie DC, Ferster D (2000) The contribution of noise to contrast invariance of orientation tuning in cat visual cortex. Science 290: 1968–1972.

Brunel N, Chance F, Fourcaud N, Abbott L (2001) Effects of synaptic noise and filtering on the frequency response of spiking neurons. Phys. Rev. Lett. 86: 2186–2189.

Brunel N, Hakim V, Richardson M (2003) Firing rate resonance in a generalized integrate-and-fire neuron with subthreshold resonance. Phys. Rev. E 67: 051916.

Brunel N, Latham P (2003) Firing rate of noisy quadratic integrate-and-fire neurons. Neural Comput. 15: 2281–2306.

Brunel N, Sergi S (1998) Firing frequency of integrate-and-fire neurons with finite synaptic time constants. J. Theor. Biol. 195: 87–95.

Destexhe A, Paré D (1999) Impact of network activity on the integrative properties of neocortical pyramidal neurons *in vivo*. J. Neurophysiol. 81: 1531–1547.

Ermentrout B (1998) Linearization of F-I curves by adaptation. Neural Comput 10: 1721–1729.

Ermentrout B, Pascal M, Gutkin B (2001) The effects of spike frequency adaptation and negative feedback on the synchronization of neural oscillators. Neural Comput. 13: 1285–310.

Ermentrout GB (1996) Type I membranes, phase resetting curves, and synchrony. Neural Comput. 8: 979–1001.

Ermentrout GB, Kopell N (1986) Parabolic bursting in an excitable system coupled with a slow oscillation. SIAM J. Appl. Math. 46: 233–253.

Fourcaud N, Brunel N (2002) Dynamics of firing probability of noisy integrate-and-fire neurons. Neural Comput. 14: 2057–2110.

Fourcaud-Trocmé N, Hansel D, van Vreeswijk C, Brunel N (2003) How spike generation mechanisms determine the neuronal response to fluctuating inputs. J. Neurosci. 23: 11628–11640.

Fuhrmann G, Markram H, Tsodyks M (2002) Spike frequency adaptation and neocortical rhythms. J. Neurophysiol. 88: 761–770.

Gerstner W (2000) Population dynamics of spiking neurons: Fast transients, asynchronous states, and locking. Neural Comput. 12: 43–89.

Gerstner W, Kistler WM (2002) Spiking Neuron Models: Single Neurons, Populations, Plasticity. Cambridge University Press.

Gutkin B, Ermentrout GB (1998) Dynamics of membrane excitability determine interspike interval variability: A link between spike generation mechanisms and cortical spike train statistics. Neural Comp. 10: 1047–1065.

Hansel D, Mato G (2003) Asynchronous states and the emergence of synchrony in large networks of interacting excitatory and inhibitory neurons. Neural Comp. 15: 1–56.

Izhikevich EM (2001) Resonate-and-fire neurons. Neural Networks 14: 883–894.

Izhikevich EM (2003) Simple model of spiking neurons. IEEE Transactions on Neural Networks 14: 1569–1572.

Knight BW (1972) Dynamics of encoding in a population of neurons. J. Gen. Physiol. 59: 734–766.

Koendgen H, Geisler C, Wang XJ, Fusi S, Luescher HR, Giugliano M (2004) The dynamical response of single cells to noisy time-varying currents. In: Society for Neuroscience Abstracts, pp. 640.9.

La Camera G, Rauch A, Luscher HR, Senn W, Fusi S (2004) Minimal models of adapted neuronal responses to *in-vivo* like input currents. Neural Comp. 16: 2101–2124.

Lapicque L (1907) Recherches quantitatives sur l'excitabilité électrique des nerfs traitée comme une polarisation. J. Physiol. Pathol. Gen. 9: 620–635.

Lindner B, Longtin A, Bulsara A (2003) Analytic expressions for rate and CV of a type I neuron driven by white gaussian noise. Neural Comp. 15: 1760–1787.

Lindner B, Schimansky-Geier L (2001) Transmission of noise coded versus additive signals through a neuronal ensemble. Phys. Rev. Lett. 86: 2934–2937.

Moreno R, Parga N (2004) Role of synaptic filtering on the firing response of simple model neurons. Phys. Rev. Lett. 92: 028102.

Naundorf B, Geisel T, Wolf F (2003) How fast can a neuron react to transient stimuli? preprint, xxx.lanl.gov, physics/0307135.

Naundorf B, Geisel T, Wolf F (2004) Action potential onset dynamics and the response speed of neuronal populations. preprint.

Rauch A, Camera GL, Lüscher H-R, Senn W, Fusi S (2003) Neocortical pyramidal cells respond as integrate-and-fire neurons to *in vivo*-like input currents. J. Neurophysiol. 90: 1598–1612.

Richardson M, Brunel N, Hakim V (2003) From subthreshold to firing-rate resonance. J. Neurophysiol. 89: 2538–2554.

Silberberg G, Bethge M, Markram H, Pawelzik K, Tsodyks M (2004) Dynamics of population rate code in ensemble of neocortical neurons. J. Neurophysiol. 91: 704–709.

Tateno T, Harsch A, Robinson HP (2004) Threshold firing frequency-current relationships of neurons in rat somatosensory cortex: Type 1 and type 2 dynamics. J. Neurophysiol. 92: 2283–2294.

Treves A (1993) Mean-field analysis of neuronal spike dynamics. Network 4: 259–284.

Tuckwell HC (1988) Introduction to Theoretical Neurobiology. Cambridge, University Press, Cambridge.

van Vreeswijk C, Hansel D (2001) Patterns of synchrony in neural networks with spike adaptation. Neural Comput. 13: 959–992.

Wang X-J, Buzsáki G (1996) Gamma oscillation by synaptic inhibition in a hippocampal interneuronal network model. J. Neurosci. 16: 6402–6413.